Geophysical Research Letters

RESEARCH LETTER
10.1029/2024GL110777

Revealing the Cape Verde Hotspot Track Across the Great Lakes

Zhongmin Tao[1], Aibing Li[1], Jonny Wu[1,2], and Karen M. Fischer[3]

[1]Department of Earth and Atmospheric Sciences, University of Houston, Houston, TX, USA, [2]Department of Geosciences, University of Arizona, Tucson, AZ, USA, [3]Department of Earth, Environmental, and Planetary Sciences, Brown University, Providence, RI, USA

Key Points:

- Positive radial anisotropy and circular azimuthal anisotropy in the eastern Great Lakes fit the predictions in a plume model
- Positive radial anisotropy anomalies align with the Cape Verde hotspot track from the Great Lakes to the Atlantic coast
- The long-time presence of the Cape Verde hotspot in the Great Lakes during 300–200 Ma helps set the stage for forming the lakes

Supporting Information:

Supporting Information may be found in the online version of this article.

Correspondence to:

A. Li,
ali2@uh.edu

Citation:

Tao, Z., Li, A., Wu, J., & Fischer, K. M. (2025). Revealing the Cape Verde hotspot track across the Great Lakes. *Geophysical Research Letters*, *52*, e2024GL110777. https://doi.org/10.1029/2024GL110777

Received 9 JUL 2024
Accepted 2 DEC 2024

Author Contributions:

Conceptualization: Aibing Li
Formal analysis: Zhongmin Tao
Investigation: Zhongmin Tao, Aibing Li, Karen M. Fischer
Methodology: Aibing Li
Resources: Jonny Wu
Software: Zhongmin Tao, Aibing Li
Writing – original draft: Zhongmin Tao, Aibing Li
Writing – review & editing: Aibing Li, Jonny Wu, Karen M. Fischer

Abstract Detecting old hotspot tracks in a stable continent remains challenging because of the lack of volcano chains on the surface and the fade of thermal anomalies with time. The northeastern American continent moved over the Cape Verde and the Great Meteor hotspots during 300–100 Ma. However, only the latter was confirmed by kimberlites and seismic velocity models. Our new 3D anisotropic model in northeastern America reveals strong positive radial anisotropy anomalies in the eastern Great Lakes, central Pennsylvania, and northwestern Virginia. These anomalies follow the Cape Verde hotspot track, providing the first geophysical evidence for the hotspot. A circular pattern of azimuthal anisotropy is also observed in the eastern Great Lakes and may be related to the Cape Verde plume activity. The plume was under the Great Lakes during 300–200 Ma and probably caused lithosphere thinning and low topography needed for forming the Lakes during the glacial era.

Plain Language Summary The strong and thick lithosphere of a stable continent makes it difficult for a hot mantle plume to penetrate and form a volcano chain on the surface. Low-velocity thermal anomalies in the upper mantle from the plume materials also fade with time and, therefore, cannot be a reliable feature for detecting an old plume path. Our new 3D seismic anisotropy model in northeastern America reveals positive radial-anisotropy anomalies in the eastern Great Lakes, central Pennsylvania, and northwestern Virginia, aligning with the Cape Verde hotspot track. A circular azimuthal anisotropy in the eastern Great Lakes may also be related to the Cape Verde plume that was under the region during 300–200 Ma. The plume activity must have thinned the lithosphere and set the stage for the birth of the Great Lakes from later glaciation.

1. Introduction

Hotspot volcanoes are thought to form above regions of anomalously hot mantle and often form age-progressive, track-like chains within oceanic plates (e.g., Hawaii). However, identifying hotspot tracks on a stable continent is far more challenging because the complex continental lithosphere structure minimizes the formation of linear volcanic chains on the surface. Northeastern North America passed over the Cape Verde (CV) and the Great Meteor (GM) hotspots during the Mesozoic and Cenozoic, according to plate reconstructions (Morgan, 1983; Müller et al., 2022). The GM hotspot track has been identified in the period of 150–115 Ma using kimberlites, Cretaceous volcanism, and other geologic and geophysical data in southeastern Canada and New England (Crough, 1981; Heaman et al., 2004; McHone & Butler, 1984; Sleep, 1990), extending to the New England seamounts in the Atlantic Ocean (Duncan, 1984) (Figure 1). However, the CV hotspot track in the North American continent has not been studied much or confirmed by geological or geophysical observations. Our anisotropic velocity model from this research provides the first evidence for the CV hotspot track in the North American continent. The coincidence of the CV hotspot with the Great Lakes suggests that the hotspot may have played a critical role in forming the most extensive freshwater lake system.

The GM and CV are long-lived hotspots currently active in the Atlantic Ocean (Figure 1). They are fed by deep mantle plumes, which produce hot thermal anomalies that are imaged as low-velocity regions in the upper mantle (French & Romanowicz, 2015). A broad low-velocity anomaly at 200 km depth from the Atlantic coast to the Great Lakes region (van der Lee & Frederiksen, 2005), located to the south of the GM hotspot track on the surface, is interpreted as the hotspot track in the mantle (Eaton & Frederiksen, 2007). However, this low-velocity anomaly is confined chiefly in New England in recent tomographic models, not extending to the Great Lakes region (Clouzet et al., 2018; Levin et al., 2018; Menke et al., 2016; Pollitz & Mooney, 2016; Schmandt & Lin, 2014; X.

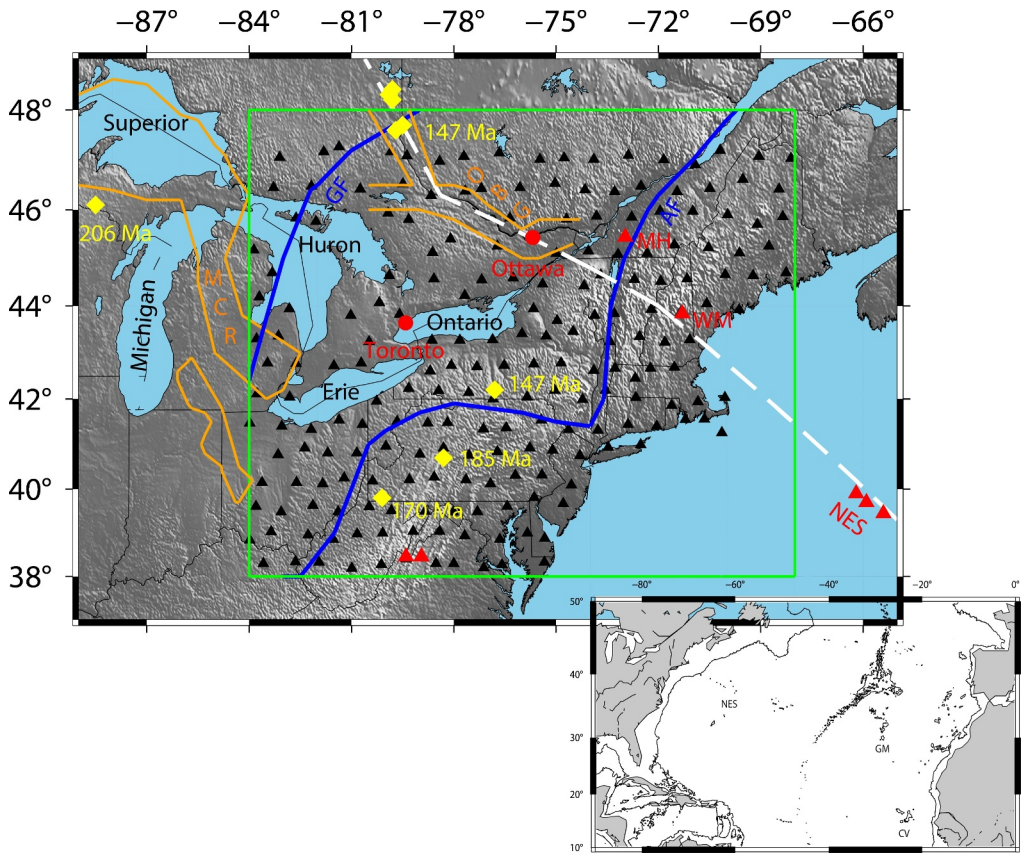

Figure 1. Map of northeastern America with tectonic features and seismic stations. The green rectangle marks the study region, and black triangles are the TA stations used in this study. Yellow diamonds are kimberlite locations. Red triangles represent the New England seamounts (NES), Cretaceous plutons in the White Mountains (WM) in New Hampshire and Monteregian Hills (MH) in Quebec, and Eocene volcanoes in northwestern Virginia. Blue curves indicate the Appalachian front and the Grenville front. The white dashed line shows the GM hotspot track. The Midcontinent Rift (MCR) and the Ottawa-Bonnechere Graben (OBG) are outlined in orange. The inset shows the current locations of the GM and CV hotspots in the Atlantic Ocean.

Yang & Gao, 2018; Yuan et al., 2011). Furthermore, a low-velocity anomaly is not a reliable feature for imaging the track of an old plume because it gradually becomes weak with time due to thermal diffusion.

Seismic anisotropy, caused by lithospheric deformation and asthenospheric flow, might be used to reveal past plume locations in continents (Tao et al., 2021) if it is frozen in the lithosphere or locked in the plume-fed sub-lithosphere mantle with high viscosity (Karato, 2008). Geodynamic simulations of plume-plate interaction have shown $V_{SH} > V_{SV}$ and circular azimuthal anisotropy in the plume head (Ito et al., 2014). However, these features only exist at a limited depth range, making it difficult to observe from seismic anisotropy measurements. These features have not been observed or investigated in previous anisotropic models (e.g., Yuan et al., 2011; Zhou et al., 2022; Zhu et al., 2017, 2020). Shear-wave splitting results (Long et al., 2016; Yang et al., 2017) have high lateral resolution but poor depth constraints of anisotropy. In this study, we have developed a high-resolution 3D anisotropic velocity model for the upper mantle of northeastern America using surface wave tomography. The model reveals distinctive positive radial-anisotropy anomalies correlating with the GM and CV hotspot tracks. A circular azimuthal anisotropy pattern in the eastern Great Lakes may also be related to the CV plume activity. These observations unveil the hidden path of the CV hotspot in the North American continent for the first time.

2. Data and Method

The surface wave data used in this study are recorded at the USArray Transportable Array (TA) in northeastern America (Figure 1 and Figure S1, and Text S1 in Supporting Information S1) with magnitude ≥5.5, focal depth ≤100 km, and epicentral distance between 25° and 120°. Fundamental mode Rayleigh and Love waves are

extracted at frequencies from 6 to 50 mHz. Both Rayleigh and Love waves show dense crossing ray paths within the station array, correlating with the area of high model resolution (Figures S2–S3 in Supporting Information S1).

A two-plane wave inversion method (Forsyth & Li, 2005; Li & Li, 2015; Y. Yang & Forsyth, 2006) is adopted to compute isotropic Rayleigh and Love wave phase velocities (Figures S4–S5, and Text S2 in Supporting Information S1), which are used in the joint inversion to construct radially anisotropic shear wave velocity models. Our anisotropic models, constrained by surface wave data from 20 to 167 s, have a high model resolution to ~250 km depth (Figure S6 and Text S3 in Supporting Information S1). We solved two independent parameters (V_{SV} and $\xi = (V_{SH}/V_{SV})^2$) using the algorithm of Saito (1988), assuming a linear relation between ξ and other anisotropic parameters (Montagner & Anderson, 1989) (Text S4 in Supporting Information S1). The initial model of the inversion is the AK135 model (Kennett et al., 1995), with the crust thickness taken from Tao et al. (2021). Rayleigh and Love wave phase velocities were directly inverted for V_{SV} and ξ, different from the procedure of Tao et al. (2021), who constrained the initial anisotropic model from isotropic V_{SV} and V_{SH} and tightly constrained the parameters in the inversion. Our new, improved radial anisotropy model reveals more details than the previous model (Tao et al., 2021) (Figures S7–S9 in Supporting Information S1).

Azimuthal anisotropic phase velocities are obtained from Rayleigh waves using the TPW method assuming a slightly anisotropic medium (Forsyth et al., 1998; Li & Detrick, 2006; Li et al., 2003; Smith & Dahlen, 1973) (Text S2 in Supporting Information S1). These anisotropic phase velocity terms, along with SKS splitting measurements at the TA stations (Figure S10 in Supporting Information S1) (Yang et al., 2017), are jointly inverted for three model parameters, V_{sv}, G_c/L, and G_s/L in each layer, where G_c, G_s, and L are linear combinations of elements in the elastic tensor C_{ijkl} (Montagner et al., 2000; Montagner & Nataf, 1986; Romanowicz & Yuan, 2012) (Text S5 in Supporting Information S1). A new 3D azimuthal anisotropy model was constructed from the joint inversion.

3. Results

3.1. Shear Wave Velocity and Radial Anisotropy Structure

The newly developed 3D anisotropic velocity model in northeastern America reveals many detailed features in the upper mantle for the first time (Figures 2 and 3, S8, S9 in Supporting Information S1). The well-known low-velocity anomaly in New England, the Northern Appalachian Anomaly (NAA), is associated with high radial anisotropy (A1). This anomaly has been interpreted as a recent asthenosphere upwelling due to edge-driven small-scale convection (Levin et al., 2018). Tao et al. (2021) associated it with past plume-lithosphere interactions that thinned the local lithosphere, leading to small-scale convection. In this paper, we focus on other anomalies in the Great Lakes region (A2), Pennsylvania (A3), Virginia, and Maryland and Delaware coast (A4) (Figure 2d).

One newly observed feature is a region of strong positive radial anisotropy in the eastern Great Lakes in the Grenville Province (A2), where velocity is not significantly low. This anomaly extends in the NE-SW direction at the uppermost mantle (Figure 2d), parallel to the Grenville front. The two ends of this anomaly fade with depth while the center remains robust to 180 km depth. High radial anisotropy regions also appear along the Ottawa-Bonnechere graben in southeastern Canada, which is a failed rift arm associated with the opening of the Iapetus Ocean ca. 590-550 Ma (Kumarapeli, 1993) (Figure 1). In the southern part of the region, high radial anisotropy anomalies are imaged in northwestern Pennsylvania near the Appalachian Front (A3), at the border of Virginia and West Virginia near the Eocene volcanoes, and the Maryland and Delaware Atlantic coast in the southeast corner of the study area. We mark the last two close anomalies as A4. Anomaly A3 correlates with a local weak low-velocity anomaly at the uppermost mantle, and anomaly A4 is associated with the Central Appalachian Anomaly (CAA) in the literature (Schmandt & Lin, 2014; Tao et al., 2021), which is right under the Eocene volcanoes in northwestern Virginia (Figures 2 and 3).

Profiles AA' and BB', crossing over significant radial-anisotropy anomalies, roughly follow the well-known GM hotspot track and the lesser-known CV hotspot track, respectively (Figure S12 in Supporting Information S1) (Morgan, 1983; Müller et al., 2022) (Movie S1). Radial anisotropy A3 and A4 are largely confined above 100 km, while A2 extends beyond 150 km depth. The observed anisotropy can be explained as the result of plume-lithosphere interaction. The lithosphere above the CV plume was heated up and became mechanically weak, and the upward pushing of plume materials extended the lithosphere radially from the plume center, generating

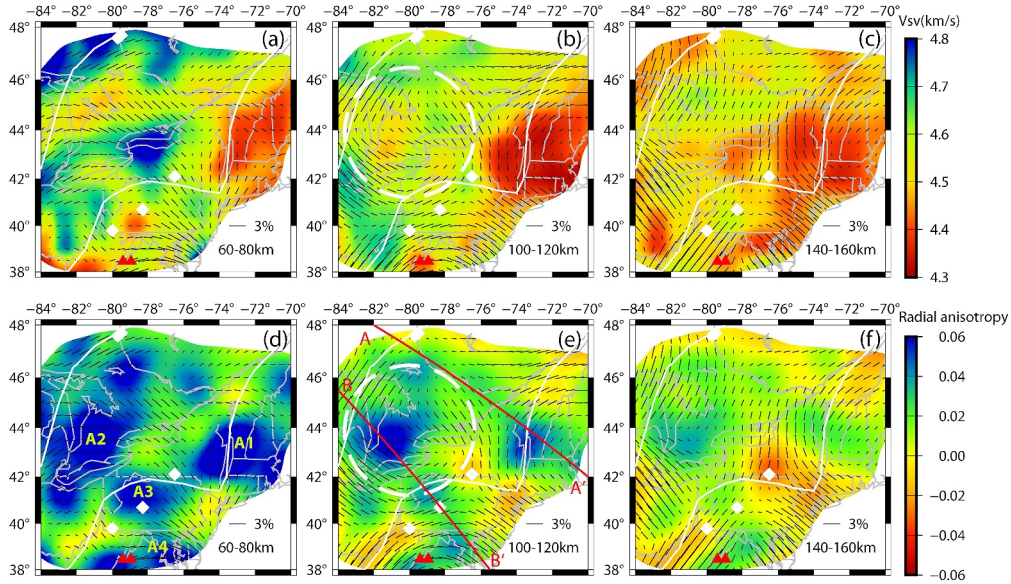

Figure 2. Maps of Vsv, radial anisotropy, and azimuthal anisotropy at selected depths. (a–c) Maps of shear wave velocity superimposed by azimuthal anisotropy (black bars). (d–f) Maps of radial anisotropy ($\xi - 1$) superimposed by azimuthal anisotropy. The bar length is proportional to the strength of azimuthal anisotropy; the bar orientation is the fast propagation direction of the S wave. White diamonds are the kimberlite locations. Red lines mark the locations of the vertical profiles AA' and BB' shown in Figure 3. The dashed white circle marks the area of circular azimuthal anisotropy. A1–A4 mark positive radial anisotropy regions.

V_{SH} > Vsv anisotropy. In the plume head beneath the lithosphere, the horizontally outward flow produced significant V_{SH} > Vsv anisotropy as demonstrated in numerical modeling (Ito et al., 2014).

The V_{SH} > Vsv anisotropy contradicts the expected V_{SV} > V_{SH} in the plume stem due to active upwelling flow. However, the plume stem in the asthenosphere continuously experienced shear from regional flow after the place

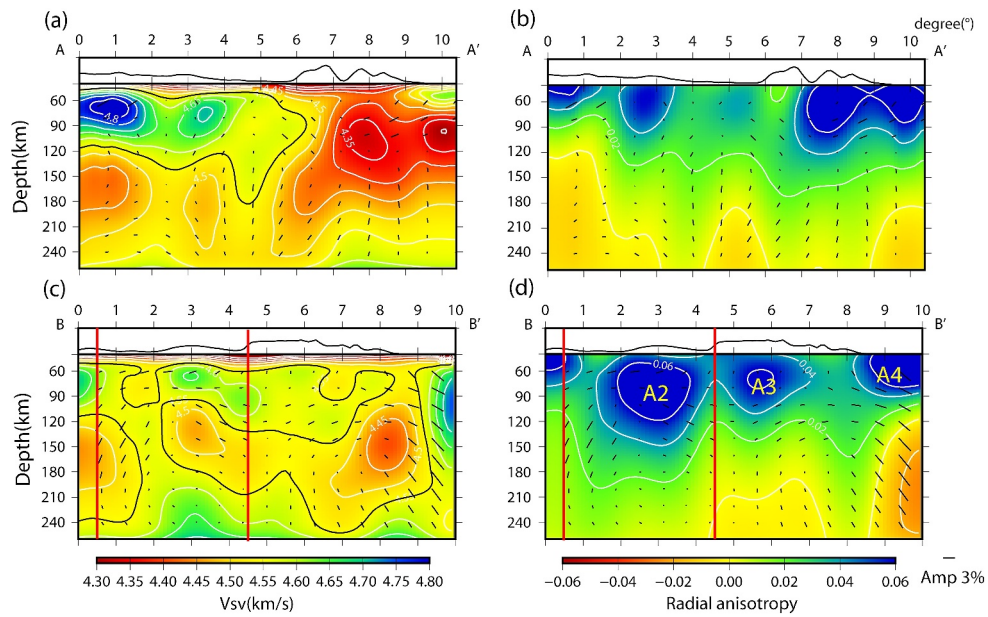

Figure 3. Vertical profiles of the anisotropic velocity model for AA' (a) and (b) and BB' (c) and (d). (a) and (c) show velocity (color) and azimuthal anisotropy (bars). (b) and (d) show radial anisotropy ($\xi - 1$) (color) and azimuthal anisotropy. The bars are plotted in a map view, with the top for north and the right for east. Black lines in (a) and (c) mark the 4.55 km/s Vsv contour.

moved away from the deep plume, resulting in $V_{SH} > V_{SV}$ anisotropy. Such anisotropy is also observed under the Hawaii hotspot track and the Afar and other African plumes (Kustowski et al., 2008; Panning & Romanowicz, 2006; Sicilia et al., 2008). In addition, Karato (2008) proposed that the $V_{SH} > V_{SV}$ anisotropy could be caused by olivine A-type fabric due to the depletion of water in plume-fed materials through partial melting. The water depletion also increases the viscosity of the plume-fed asthenosphere and helps preserve the anisotropy.

3.2. Azimuthal Anisotropy Structure

Azimuthal anisotropy shows substantial 3D variations in strength and fast direction (Figures 2, 3, S9, S11 in Supporting Information S1). Our area of interest is the eastern Great Lakes region between the Appalachian and the Grenville where the radial-anisotropy anomaly A2 is imaged. It is also at the center of the study area where model resolution is high. Anisotropy at 40–100 km depths is complex, with fast directions varying in EW, NW-SE, and NE-SW, which are mostly inconsistent with the Grenville and Appalachian orogenic belts. These complex fast directions are also observed from SKS splitting data in this area (Fouch et al., 2000; Long et al., 2016; Yang et al., 2017), suggesting the fabrics associated with the past orogenies have been overprinted by later tectonic events.

A noticeable change in azimuthal anisotropy occurs at 100–140 km, revealing a circular pattern with weak anisotropy at the center, coincident with the high radial anisotropy A2 in the eastern Great Lakes (Figures 2 and 3, S9, and S11 in Supporting Information S1). Considering the last major tectonic event here is the CV plume activity at ∼215 Ma (Müller et al., 2022), this circular azimuthal anisotropy could be formed in the plume head due to circumferential stretching of the plume materials that flew radially outward from the plume stem (Druken et al., 2013; Ito et al., 2014). The anisotropy could be preserved if the plume head became more viscous due to cooling after the area moved away from the plume. Furthermore, the viscosity in the plume head could be increased by the depletion of water through partial melting (Karato, 2008).

Alternatively, the circular azimuthal anisotropy could be formed more recently and produced by guided asthenosphere flow in a lithosphere cavity. The present lithosphere-asthenosphere boundary (LAB) in the eastern Great Lakes is not defined by receiver functions (Hopper & Fischer, 2018). The 4.55 km/s Vsv contour in Figure 3c outlines a weak low-velocity layer across profile BB'. The top boundary of the layer is shallower under anomaly A2, indicating a thinner lithosphere. The original thick Proterozoic lithosphere here may have been delaminated due to thermal erosion or metasomatism by the CV plume, forming a cavity at the base of the lithosphere. Regional asthenosphere flow could be guided by the curved boundary of the indented cavity, producing this circular azimuthal anisotropy.

4. Discussion

4.1. The Hotspot Tracks in Northeastern America

Plate reconstructions show that the broad Great Lakes region passed over the CV hotspot at 300-200 Ma and the GM hotspot at ∼150 Ma (Morgan, 1983; Müller et al., 2022) (Figure S12 in Supporting Information S1 and Movie S1). The GM hotspot track has been well-mapped using NW-SE trending and southeast-younging Jurassic kimberlites (Heaman et al., 2004; Heaman & Kjarsgaard, 2000) and early Cretaceous plutons from Quebec to New England (McHone & Butler, 1984). This track follows the Ottawa-Bonnechere graben and reaches to the New England seamounts (Figure 1). The GM hotspot has been frequently associated with geophysical observations, such as low-velocity anomalies in northeastern America (Eaton & Frederiksen, 2007; Li et al., 2003; Pollitz & Mooney, 2016; Schmandt & Lin, 2014; Tao et al., 2021).

The kimberlites in Michigan, Pennsylvania, and New York (Figure 4a) also show a general southeast-younging trend, with the oldest ages of 206 Ma at Lake Ellen in Michigan, intermediate ages of 185–175 Ma in Pennsylvania, and youngest ages of 146 Ma in Ithaca in New York. Their age progression suggests they are probably related to the CV hotspot (Müller et al., 2022). However, the nonlinear distribution of these kimberlites does not explicitly indicate a hotspot track. Numerical simulations have shown that magmatism in continental settings from a mantle plume is complex since the flow of plume materials is mainly controlled by the variations of lithosphere structure (Duvernay et al., 2022). The 206 Ma kimberlite in Michigan and the 185 and 170 Ma kimberlites in Pennsylvania generally agree with the CV hotspot track. The 147 Ma kimberlite in southern New York is off the track and too young to be directly associated with the CV hotspot. It could be caused by small-scale

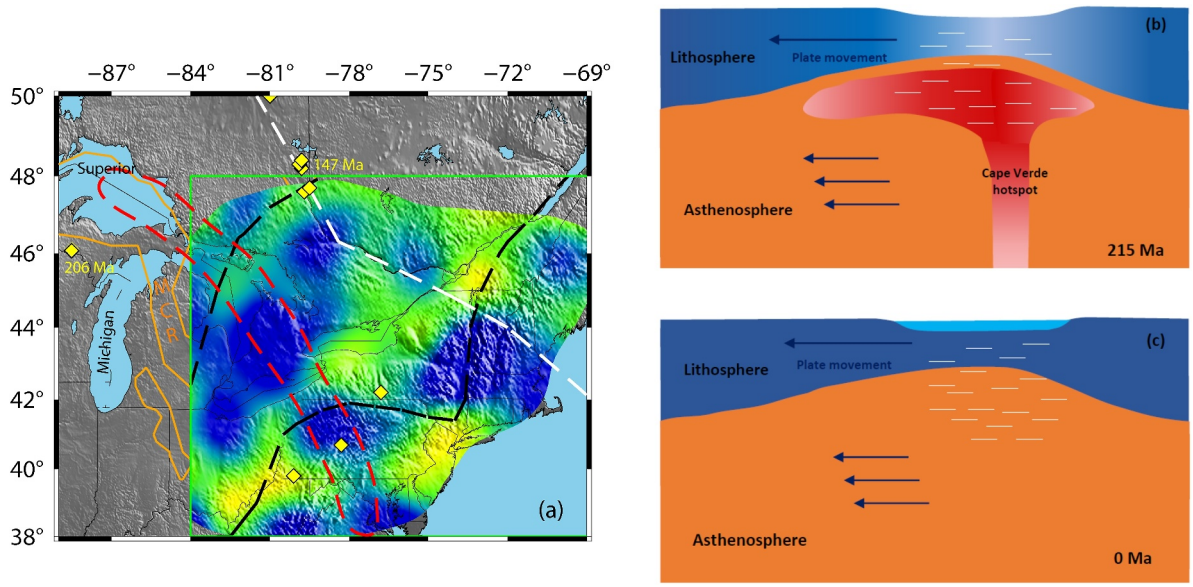

Figure 4. The proposed CV hotspot track and mechanism for forming the Great Lakes from plume-lithosphere interaction. (a) The radial anisotropy map at 60–80 km depths (Figure 2d) showing the possible CV hotspot track outlined by the red dashed line (Müller et al., 2022) and its correlation with radial anisotropy anomalies and Kimberlite locations (yellow diamonds). The white dashed line indicates the GM hotspot track. (b) Cartoon showing the CV plume actively interacted with the lithosphere in the eastern Great Lakes at 215 Ma, causing lithosphere thinning. Arrows indicate the plate motion and regional asthenosphere flow. (c) The current stage of the lithosphere under the eastern Great Lakes, corresponding to the segment marked by two red lines on profile BB' (Figure 3). The thinning of the lithosphere by the CV plume activity caused the low topography of the region, leading to the formation of the Great Lakes by later glaciation.

mantle convection triggered by lithosphere thickness change caused by the plume interaction (Crough et al., 1980; Kjarsgaard et al., 2017).

The CV hotspot track is quite complex according to the model by Müller et al. (2022) (Figure S12 in Supporting Information S1 and Movie S1). The hotspot was primarily under Lake Superior at 300–225 Ma when the supercontinent Pangea was almost stationary. From 225 to 205 Ma, the hotspot track followed the western boundary of Lake Huron to Lake Erie. Then, the track headed southeastward across Pennsylvania and northern Virginia, intersecting the coastline around 170 Ma. Unlike the GM hotspot, the CV hotspot track has not been associated with geophysical observations, maybe because the CV hotspot was much older than the GM hotspot, and any related thermal anomaly probably has dissipated over time. Interestingly, the imaged radial anisotropy anomalies in the eastern Great Lakes region, central Pennsylvania, and northwestern Virginia (Figure 4a) are all on the CV hotspot track. The deeply buried path of the ancient CV hotspot is revealed for the first time in our new anisotropic velocity model.

4.2. New Insights Into Past Heating Events

Although Morgan (1983) proposed the CV hotspot track in the North American continent more than four decades ago, its influence on local geology is rarely studied in the literature. Apatite fission track analysis and organic maturity data (Cercone, 1984; Cercone & Pollack, 1991; Crowley, 1991) indicated a Late Paleozoic and Early Triassic heating event in the Michigan Basin, a nearly circular region between Lake Michigan and Lake Huron, which could be easily interpreted by the increase in heat flow. However, this interpretation was not favored because the source of the excess heat from the basement was unknown (Cercone & Pollack, 1991; Crowley, 1991). Instead, previous studies preferred other mechanisms, such as sediment burial. The presence of the CV hotspot during 300–200 Ma in the Great Lakes region provides a simple explanation for the observed heating, uplift, and erosion in the Michigan Basin from geological observations (Cercone, 1984; Cercone & Pollack, 1991; Crowley, 1991).

The identified CV hotspot track also helps explain the central Appalachian low-velocity anomaly (CCA) in northern Virginia and West Virginia, coincident with radial anisotropy anomaly A4 (Figure 2) (Chu et al., 2013; Long, 2024; Long et al., 2021; Schmandt & Lin, 2014; Tao et al., 2021; Wagner et al., 2018). The CCA correlates

with the youngest magma eruption of ∼48 Ma in the eastern North American margin (Mazza et al., 2014, 2017) (Figure 1). The origin of the CCA has been interpreted as a hidden hotspot track (Chu et al., 2013; Tao et al., 2021) or as asthenospheric upwelling due to lithosphere delamination (Long et al., 2021; Mazza et al., 2014). The new results of this study show that the CAA is on the CV hotspot track, which is different from the unknown hotspot proposed in previous studies (Chu et al., 2013; Tao et al., 2021). However, the Eocene magma eruption cannot be directly caused by the CV hotspot, which was under the region approximately 130 My earlier. They were more likely caused by small-scale mantle convection due to lithosphere thickness variations caused by the CV plume (King & Anderson, 1998; van Wijk et al., 2010). Furthermore, the connection between the CCA and the CV hotspot track helps elucidate a paradox of similar isotopic signatures in Virginia Eocene volcanoes and the current CV hotspot in the Atlantic Ocean (Figure 1) (Mazza et al., 2014) because the upper mantle beneath the CAA could have been intruded by the CV plume materials during the Jurassic.

4.3. The Formation of the Great Lakes

The Great Lakes in North America are the largest group of freshwater lakes on Earth, and the processes that produce such an enormous waterbody in the middle of a stable continent is a critical question for planetary evolution. The origin of the Great Lakes has been mainly attributed to Quaternary glaciations when ice flow scoured and eroded relatively weak rocks along preglacial bedrock valleys (Hough, 1958; Larson & Schaetzl, 2001). The area before the Quaternary glaciations must have lower topography than its surroundings to form the Great Lakes. However, there is no strong evidence for the proposed proto-Great Lakes valley systems before the Quaternary glaciations (Larson & Schaetzl, 2001). Another possibility is the impact of the two failed continental rift systems that exist in the vicinity of the Great Lakes, the ∼1.1 Ga Midcontinent Rift (MCR), which is a horseshoe-shaped band centered at Lake Superior (Stein et al., 2016, 2018), and the ∼590 Ma Ottawa-Bonnechere and Timiskaming Graben, which is a failed arm of the Iapetus Ocean at (Kumarapeli, 1993) (Figure 1). However, the lakes do not overlap with the rift arms, except for Lake Superior.

Our anisotropic model provides geophysical evidence for the CV mantle plume under the Great Lakes region, agreeing with a recent plate reconstruction model (Müller et al., 2022). Here we propose that the CV hotspot must have played a fundamental role in setting the stage for developing the Great Lakes (Figure 4). The hotspot interacted with the lithosphere at the Great Lakes region during 300–200 Ma, indicating the super-continent Pangea was nearly stationary or moving very slowly at that time. A possible modern analogy is the slow-moving African continent pinned by the Afar plume (Burke & Dewey, 1973), causing the continent to rupture in three rifts and forming the Afar triple junction. Similarly, Lake Superior, Michigan, and Huron might be viewed as three rifting arms above the ancient CV hotspot during its 100-My interaction with the North American continent in the Great Lakes region. The relatively thin crust under Lake Huron and Michigan and the high-velocity lower crust (Schmandt et al., 2015) provide evidence for plume-related crustal thinning and magmatic underplating. The lithosphere, if defined by the top boundary of the low-velocity layer, is thinner under the eastern Great Lakes than under the Appalachians (Figure 3c), confirming the influence of the CV plume.

The interaction between a mantle plume and a stable continent can produce extension, complex magmatic intrusion, and variable surface uplift (Guillou-Frottier et al., 2007). Although the unmodified cratonic lithosphere is unlikely to be disrupted by a single plume event, it can be thinned if the cratonic root has been modified by fluid-melt metasomatism (Wang et al., 2015). For example, widespread lithosphere erosion is observed in the cratons in Africa (Celli et al., 2020). Since the Great Lakes region partially overlaps the MCR, the lithosphere must have been significantly weakened by the rifting event, making it susceptible to thermal erosion by the CV plume, especially when the interaction is about 100 My long. After the Great Lakes lithosphere moved away from the CV hotspot, the high-elevation region from plume buoyance would have continued to subside over hundreds of millions of years. This subsidence, combined with the lower buoyancy of thinner crust with a more mafic composition, would have caused portions of the region to stand lower. This proposed scenario is based on physical conceptions, while accurate modeling of past plume-lithosphere interaction is beyond the scope of this study. These low-lying regions initiated by the CV hotspot could have set the stage for the birth of the Great Lakes during Quaternary glaciations. Thus, the Great Lakes probably demonstrate a powerful combination of deep Earth and climate processes over long timescales.

Conflict of Interest

The authors declare no conflicts of interest relevant to this study.

Data Availability Statement

The earthquake data are obtained using the Interactive Earthquake Brower from the IRIS (http://ds.iris.edu/ieb/). The USArray TA station locations are downloaded at (https://ds.iris.edu/ds/nodes/dmc/earthscope/usarray/_US-TA/). We requested seismograms for the selected events and stations by sending emails to breq_fast@iris.washington.edu. The instructions for using BREQ_FAST to request data can be found at https://ds.iris.edu/ds/nodes/dmc/manuals/breq_fast/. Shear-wave splitting measurements are from Yang et al. (2017). Most figures are made using the Generic Mapping Tools (https://www.generic-mapping-tools.org/) (Wessel et al., 2019).

Acknowledgments
We used the earthquake data recorded by the USArray Transportable Array stations that are available from the Incorporated Research Institutions for Seismology (IRIS). Shear-wave splitting measurements from Yang et al. (2017) are also downloaded from the IRIS. We are grateful to Stephen Gao, two anonymous reviewers, and editor Daoyuan Sun for providing insightful comments that helped improve this manuscript. This project is supported by National Science Foundation Grants EAR-1614860.

References

Burke, K., & Dewey, J. F. (1973). Plume-generated triple junctions: Key indicators in applying plate tectonics to old rocks. *The Journal of Geology*, *81*(4), 406–433. https://doi.org/10.1086/627882

Celli, N. L., Lebedev, S., Schaeffer, A. J., & Gaina, C. (2020). African cratonic lithosphere carved by mantle plumes. *Nature Communications*, *11*(1), 92. https://doi.org/10.1038/s41467-019-13871-2

Cercone, K. R. (1984). Thermal history of Michigan basin. *AAPG Bulletin*, *68*(2), 130–136. https://doi.org/10.1306/ad4609e5-16f7-11d7-8645000102c1865d

Cercone, K. R., & Pollack, H. N. (1991). Thermal maturity of the Michigan basin. *Geological Society of America Special Paper*, *256*, 1–11. https://doi.org/10.1130/SPE256-p1

Chu, R., Leng, W., Helmberger, D. V., & Gurnis, M. (2013). Hidden hotspot track beneath the eastern United States. *Nature Geoscience*, *6*(11), 963–966. https://doi.org/10.1038/ngeo1949

Clouzet, P., Masson, Y., & Romanowicz, B. (2018). Box tomography: First application to the imaging of upper-mantle shear velocity and radial anisotropy structure beneath the North American continent. *Geophysical Journal International*, *213*(3), 1849–1875. https://doi.org/10.1093/gji/ggy078

Crough, S. T. (1981). Mesozoic hotspot epeirogeny in eastern North America. *Geology*, *9*(1), 2–6. https://doi.org/10.1130/0091-7613(1981)9<2:MHEIEN>2.0.CO;2

Crough, S. T., Morgan, W. J., & Hargraves, R. B. (1980). Kimberlites: Their relation to mantle hotspots. *Earth and Planetary Science Letters*, *50*(1), 260–274. https://doi.org/10.1016/0012-821X(80)90137-5

Crowley, K. D. (1991). Thermal history of Michigan Basin and Southern Canadian Shield from apatite fission track analysis. *Journal of Geophysical Research*, *96*(B1), 697–711. https://doi.org/10.1029/90JB02174

Druken, K. A., Kincaid, C., & Griffiths, R. W. (2013). Directions of seismic anisotropy in laboratory models of mantle plumes. *Geophysical Research Letters*, *40*(14), 3544–3549. https://doi.org/10.1002/grl.50671

Duncan, R. A. (1984). Age progressive volcanism in the New England seamounts and the opening of the central Atlantic Ocean. *Journal of Geophysical Research*, *89*(B12), 9980–9990. https://doi.org/10.1029/JB089iB12p09980

Duvernay, T., Davies, D. R., Mathews, C. R., Gibson, A. H., & Kramer, S. C. (2022). Continental magmatism: The surface manifestation of dynamic interactions between cratonic lithosphere, mantle plumes and edge-driven convection. *Geochemistry, Geophysics, Geosystems*, *23*(7), e2022GC010363. https://doi.org/10.1029/2022gc010363

Eaton, D. W., & Frederiksen, A. (2007). Seismic evidence for convection-driven motion of the North American plate. *Nature*, *446*(7134), 428–431. https://doi.org/10.1038/nature05675

Forsyth, D. W., & Li, A. (2005). Array analysis of two-dimensional variations in surface wave phase velocity and azimuthal anisotropy in the presence of multipathing interference. In A. Levander & G. Nolet (Eds.), *Seismic Earth: Array analysis of broadband seismograms* (Vol. 157, pp. 81–97). Geophysical Monograph-American Geophysical Union. https://doi.org/10.1029/157gm06

Forsyth, D. W., Webb, S. C., Dorman, L. M., & Shen, Y. (1998). Phase velocities of Rayleigh waves in the MELT experiment on the east Pacific rise. *Science*, *280*(5367), 1235–1238. https://doi.org/10.1126/science.280.5367.1235

Fouch, M. J., Fischer, K. M., Parmentier, E. M., Wysession, M. E., & Clarke, T. J. (2000). Shear wave splitting, continental keels, and patterns of mantle flow. *Journal of Geophysical Research*, *105*(B3), 6255–6275. https://doi.org/10.1029/1999JB900372

French, S. W., & Romanowicz, B. (2015). Broad plumes rooted at the base of the Earth's mantle beneath major hotspots. *Nature*, *525*(7567), 95–99. https://doi.org/10.1038/nature14876

Guillou-Frottier, L., Burov, E., Nehlig, P., & Wyns, R. (2007). Deciphering plume–lithosphere interactions beneath Europe from topographic signatures. *Global and Planetary Change*, *58*(1–4), 119–140. https://doi.org/10.1016/j.gloplacha.2006.10.003

Heaman, L. M., & Kjarsgaard, B. A. (2000). Timing of eastern North American kimberlite magmatism: Continental extension of the Great meteor hotspot track? *Earth and Planetary Science Letters*, *178*(3–4), 253–268. https://doi.org/10.1016/S0012-821X(00)00079-0

Heaman, L. M., Kjarsgaard, B. A., & Creaser, R. A. (2004). The temporal evolution of North American kimberlites. *Lithos*, *76*(1–4), 377–397. https://doi.org/10.1016/j.lithos.2004.03.047

Hopper, E., & Fischer, K. M. (2018). The changing face of the lithosphere-asthenosphere boundary: Imaging continental scale patterns in upper mantle structure across the contiguous US with Sp converted waves. *Geochemistry, Geophysics, Geosystems*, *19*(8), 2593–2614. https://doi.org/10.1029/2018gc007476

Hough, J. L. (1958). *Geology of the Great lakes*. University of Illinois Press.

Ito, G., Dunn, R., Li, A., Wolfe, C. J., Gallego, A., & Fu, Y. (2014). Seismic anisotropy and shear wave splitting associated with mantle plume-plate interaction. *Journal of Geophysical Research: Solid Earth*, *119*(6), 4923–4937. https://doi.org/10.1002/2013JB010735

Karato, S. I. (2008). Insights into the nature of plume–asthenosphere interaction from central Pacific geophysical anomalies. *Earth and Planetary Science Letters*, *274*(1–2), 234–240. https://doi.org/10.1016/j.epsl.2008.07.033

Kennett, B. L., Engdahl, E. R., & Buland, R. (1995). Constraints on seismic velocities in the Earth from traveltimes. *Geophysical Journal International*, *122*(1), 108–124. https://doi.org/10.1111/j.1365-246X.1995.tb03540.x

King, S. D., & Anderson, D. L. (1998). Edge-driven convection. *Earth and Planetary Science Letters*, *160*(3–4), 289–296. https://doi.org/10.1016/S0012-821X(98)00089-2

Kjarsgaard, B. A., Heaman, L. M., Sarkar, C., & Pearson, D. G. (2017). The North America mid-Cretaceous kimberlite corridor: Wet, edge-driven decompression melting of an OIB-type deep mantle source. *Geochemistry, Geophysics, Geosystems*, *18*(7), 2727–2747. https://doi.org/10.1002/2016GC006761

Kumarapeli, P. S. (1993). A plume-generated segment of the rifted margin of Laurentia, southern Canadian Appalachians, seen through a completed Wilson cycle. *Tectonophysics*, *219*(1–3), 47–55. https://doi.org/10.1016/0040-1951(93)90286-S

Kustowski, B., Ekström, G., & Dziewoński, A. M. (2008). Anisotropic shear-wave velocity structure of the Earth's mantle: A global model. *Journal of Geophysical Research*, *113*(B6). https://doi.org/10.1029/2007jb005169

Larson, G., & Schaetzl, R. (2001). Origin and evolution of the Great lakes. *Journal of Great Lakes Research*, *27*(4), 518–546. https://doi.org/10.1016/S0380-1330(01)70665-X

Levin, V., Long, M. D., Skryzalin, P., Li, Y., & López, I. (2018). Seismic evidence for a recently formed mantle upwelling beneath New England. *Geology*, *46*(1), 87–90. https://doi.org/10.1130/G39641.1

Li, A., & Detrick, R. S. (2006). Seismic structure of Iceland from Rayleigh wave inversions and geodynamic implications. *Earth and Planetary Science Letters*, *241*(3–4), 901–912. https://doi.org/10.1016/j.epsl.2005.10.031

Li, A., Forsyth, D. W., & Fischer, K. M. (2003). Shear velocity structure and azimuthal anisotropy beneath eastern North America from Rayleigh wave inversion. *Journal of Geophysical Research*, *108*(B8). https://doi.org/10.1029/2002JB002259

Li, A., & Li, L. (2015). Love wave tomography in southern Africa from a two-plane-wave inversion method. *Geophysical Journal International*, *202*(2), 1005–1020. https://doi.org/10.1093/gji/ggv203

Long, M. D. (2024). Evolution, modification, and deformation of continental lithosphere: Insights from the eastern margin of north America. *Annual Review of Earth and Planetary Sciences*, *52*(1), 549–580. https://doi.org/10.1146/annurev-earth-040522-115229

Long, M. D., Jackson, K. G., & McNamara, J. F. (2016). SKS splitting beneath T ransportable A rray stations in eastern N orth A merica and the signature of past lithospheric deformation. *Geochemistry, Geophysics, Geosystems*, *17*(1), 2–15. https://doi.org/10.1002/2015GC006088

Long, M. D., Wagner, L. S., King, S. D., Evans, R. L., Mazza, S. E., Byrnes, J. S., et al. (2021). Evaluating models for lithospheric loss and intraplate volcanism beneath the Central Appalachian Mountains. *Journal of Geophysical Research: Solid Earth*, *126*(10), e2021JB022571. https://doi.org/10.1029/2021JB022571

Mazza, S. E., Gazel, E., Johnson, E. A., Bizimis, M., McAleer, R., & Biryol, C. B. (2017). Post-rift magmatic evolution of the eastern N orth A merican "passive-aggressive" margin. *Geochemistry, Geophysics, Geosystems*, *18*(1), 3–22. https://doi.org/10.1002/2016GC006646

Mazza, S. E., Gazel, E., Johnson, E. A., Kunk, M. J., McAleer, R., Spotila, J. A., et al. (2014). Volcanoes of the passive margin: The youngest magmatic event in eastern North America. *Geology*, *42*(6), 483–486. https://doi.org/10.1130/G35407.1

McHone, J. G., & Butler, J. R. (1984). Mesozoic igneous provinces of new England and the opening of the North Atlantic Ocean. *Geological Society of America Bulletin*, *95*(7), 757–765. https://doi.org/10.1130/0016-7606(1984)95<757:mipone>2.0.co;2

Menke, W., Skryzalin, P., Levin, V., Harper, T., Darbyshire, F., & Dong, T. (2016). The northern appalachian anomaly: A modern asthenospheric upwelling. *Geophysical Research Letters*, *43*(19), 10–173. https://doi.org/10.1002/2016gl070918

Montagner, J. P., & Anderson, D. L. (1989). Petrological constraints on seismic anisotropy. *Physics of the Earth and Planetary Interiors*, *54*(1–2), 82–105. https://doi.org/10.1016/0031-9201(89)90189-1

Montagner, J. P., Griot-Pommera, D. A., & Lavé, J. (2000). How to relate body wave and surface wave anisotropy? *Journal of Geophysical Research*, *105*(B8), 19015–19027. https://doi.org/10.1029/2000JB900015

Montagner, J. P., & Nataf, H. C. (1986). A simple method for inverting the azimuthal anisotropy of surface waves. *Journal of Geophysical Research*, *91*(B1), 511–520. https://doi.org/10.1029/JB091iB01p00511

Morgan, W. J. (1983). Hotspot tracks and the early rifting of the Atlantic. *Developments in Geotectonics*, *19*, 123–139. https://doi.org/10.1016/B978-0-444-42198-2.50015-8

Müller, R. D., Flament, N., Cannon, J., Tetley, M. G., Williams, S. E., Cao, X., et al. (2022). A tectonic-rules-based mantle reference frame since 1 billion years ago–implications for supercontinent cycles and plate–mantle system evolution. *Solid Earth*, *13*(7), 1127–1159. https://doi.org/10.5194/se-13-1127-2022

Panning, M., & Romanowicz, B. (2006). A three-dimensional radially anisotropic model of shear velocity in the whole mantle. *Geophysical Journal International*, *167*(1), 361–379. https://doi.org/10.1111/j.1365-246x.2006.03100.x

Pollitz, F. F., & Mooney, W. D. (2016). Seismic velocity structure of the crust and shallow mantle of the Central and Eastern United States by seismic surface wave imaging. *Geophysical Research Letters*, *43*(1), 118–126. https://doi.org/10.1002/2015GL066637

Romanowicz, B., & Yuan, H. (2012). On the interpretation of SKS splitting measurements in the presence of several layers of anisotropy. *Geophysical Journal International*, *188*(3), 1129–1140. https://doi.org/10.1111/j.1365-246X.2011.05301.x

Saito, M. (1988). DISPER80: A subroutine package for the calculation of seismic normal-mode solutions. In D. Doornbos (Ed.), *Seismological algorithms: Computational methods and computer programs* (pp. 293–319). Elsevier.

Schmandt, B., & Lin, F. C. (2014). P and S wave tomography of the mantle beneath the United States. *Geophysical Research Letters*, *41*(18), 6342–6349. https://doi.org/10.1002/2014GL061231

Schmandt, B., Lin, F. C., & Karlstrom, K. E. (2015). Distinct crustal isostasy trends east and west of the Rocky Mountain Front. *Geophysical Research Letters*, *42*(23), 10–290. https://doi.org/10.1002/2015GL066593

Sicilia, D., Montagner, J. P., Cara, M., Stutzmann, E., Debayle, E., Lépine, J. C., et al. (2008). Upper mantle structure of shear-waves velocities and stratification of anisotropy in the Afar Hotspot region. *Tectonophysics*, *462*(1–4), 164–177. https://doi.org/10.1016/j.tecto.2008.02.016

Sleep, N. H. (1990). Monteregian hotspot track: A long-lived mantle plume. *Journal of Geophysical Research*, *95*(B13), 21983–21990. https://doi.org/10.1029/JB095iB13p21983

Smith, M. L., & Dahlen, F. A. (1973). The azimuthal dependence of Love and Rayleigh wave propagation in a slightly anisotropic medium. *Journal of Geophysical Research*, *78*(17), 3321–3333. https://doi.org/10.1029/JB078i017p03321

Stein, S., Stein, C. A., Elling, R., Kley, J., Keller, G. R., Wysession, M. E., et al. (2018). Insights from North America's failed Midcontinent Rift into the evolution of continental rifts and passive continental margins. *Tectonophysics*, *744*, 403–421. https://doi.org/10.1016/j.tecto.2018.07.021

Stein, S., Stein, C. A., Kley, J., Keller, G. R., Merino, M., Wolin, E., et al. (2016). New insights into North America's Midcontinent rift. *Eos*, *97*. https://doi.org/10.1029/2016EO056659

Tao, Z., Li, A., & Fischer, K. M. (2021). Hotspot signatures at the North American passive margin. *Geology*, *49*(5), 525–530. https://doi.org/10.1130/G47994.1

van der Lee, S., & Frederiksen, A. (2005). Surface wave tomography applied to the North American upper mantle. *Washington DC American Geophysical Union Geophysical Monograph Series*, *157*, 67–80. https://doi.org/10.1029/157GM05

van Wijk, J. W., Baldridge, W. S., Van Hunen, J., Goes, S., Aster, R., Coblentz, D. D., et al. (2010). Small-scale convection at the edge of the Colorado Plateau: Implications for topography, magmatism, and evolution of Proterozoic lithosphere. *Geology*, *38*(7), 611–614. https://doi.org/10.1130/G31031.1

Wagner, L. S., Fischer, K. M., Hawman, R., Hopper, E., & Howell, D. (2018). The relative roles of inheritance and long-term passive margin lithospheric evolution on the modern structure and tectonic activity in the southeastern United States. *Geosphere*, *14*(4), 1385–1410. https://doi.org/10.1130/GES01593.1

Wang, H., van Hunen, J., & Pearson, D. G. (2015). The thinning of subcontinental lithosphere: The roles of plume impact and metasomatic weakening. *Geochemistry, Geophysics, Geosystems*, *16*(4), 1156–1171. https://doi.org/10.1002/2015GC005784

Wessel, P., Luis, J. F., Uieda, L., Scharroo, R., Wobbe, F., Smith, W. H. F., & Tian, D. (2019). The generic mapping tools version 6. *Geochemistry, Geophysics, Geosystems*, *20*(11), 5556–5564. https://doi.org/10.1029/2019GC008515

Yang, B. B., Liu, Y., Dahm, H., Liu, K. H., & Gao, S. S. (2017). Seismic azimuthal anisotropy beneath the eastern United States and its geodynamic implications. *Geophysical Research Letters*, *44*(6), 2670–2678. https://doi.org/10.1002/2016GL071227

Yang, X., & Gao, H. (2018). Full-wave seismic tomography in the northeastern United States: New insights into the uplift mechanism of the Adirondack Mountains. *Geophysical Research Letters*, *45*(12), 5992–6000. https://doi.org/10.1029/2018gl078438

Yang, Y., & Forsyth, D. W. (2006). Regional tomographic inversion of the amplitude and phase of Rayleigh waves with 2-D sensitivity kernels. *Geophysical Journal International*, *166*(3), 1148–1160. https://doi.org/10.1029/2005JB004180

Yuan, H., Romanowicz, B., Fischer, K. M., & Abt, D. (2011). 3-D shear wave radially and azimuthally anisotropic velocity model of the North American upper mantle. *Geophysical Journal International*, *184*(3), 1237–1260. https://doi.org/10.1111/j.1365-246X.2010.04901.x

Zhou, T., Li, J., Xi, Z., Li, G., & Chen, M. (2022). CUSRA2021: A radially anisotropic model of the contiguous US and surrounding regions by full-waveform inversion. *Journal of Geophysical Research: Solid Earth*, *127*(8), e2021JB023893. https://doi.org/10.1029/2021JB023893

Zhu, H., Komatitsch, D., & Tromp, J. (2017). Radial anisotropy of the North American upper mantle based on adjoint tomography with USArray. *Geophysical Journal International*, *211*(1), 349–377. https://doi.org/10.1093/gji/ggx305

Zhu, H., Yang, J., & Li, X. (2020). Azimuthal anisotropy of the North American upper mantle based on full waveform inversion. *Journal of Geophysical Research: Solid Earth*, *125*(2), e2019JB018432. https://doi.org/10.1029/2019JB018432

References From the Supporting Information

Dziewonski, A. M., & Anderson, D. L. (1981). Preliminary reference Earth model. *Physics of the Earth and Planetary Interiors*, *25*(4), 297–356. https://doi.org/10.1016/0031-9201(81)90046-7

Takeuchi, H., & Saito, M. (1972). Seismic surface waves. *Methods in Computational Physics*, *11*, 217–295. https://doi.org/10.1016/b978-0-12-460811-5.50010-6

Tao, Z. (2022). *Anisotropic seismic velocity in the crust and upper mantle of northeastern America from surface wave tomography*. University of Houston. Retrieved from https://hdl.handle.net/10657/14304